

**A major purpose of the Technical Information Center is to provide the broadest dissemination possible of information contained in DOE's Research and Development Reports to business, industry, the academic community, and federal, state and local governments.**

**Although a small portion of this report is not reproducible, it is being made available to expedite the availability of information on the research discussed herein.**

**1**

CONF-8312LS-1

LA-UR--84-202

DE84 006024

**NOTICE**  
**PORTIONS OF THIS REPORT ARE ILLEGIBLE.**  
It has been reproduced from the best available copy to permit the broadest possible availability.

Los Alamos National Laboratory is operated by the University of California for the United States Department of Energy under contract number AC05-84OR21400

**TITLE FIRST OPERATION OF THE LOS ALAMOS FREE-ELECTRON LASER OSCILLATOR**

**AUTHORS:** R. W. Warren, B. E. Newnam, H. E. Stein, J. G. Winston, R. L. Sheffield, M. T. Lynch, J. C. Goldstein, M. C. Whitehead, O. R. Norris, G. Luedemarn, T. O. Gibson, and C. M. Humphry

**SUBMITTED TO** Sixth International Conference on Lasers & Applications, LASERS '83, San Francisco, CA December 13-16, 1983. Sponsored by Society for Optical and Quantum Electronics

**DISCLAIMER**

This report was prepared as an account of work sponsored by an agency of the United States Government. Neither the United States Government nor any agency thereof, nor any of their employees, makes any warranty, express or implied, or assumes any legal liability or responsibility for the accuracy, completeness, or usefulness of any information, apparatus, product, or process disclosed, or represents that its use would not infringe privately owned rights. Reference herein to any specific commercial product, process, or service by trade name, trademark, manufacturer, or otherwise does not necessarily constitute or imply its endorsement, recommendation, or favoring by the United States Government or any agency thereof. The views and opinions of authors expressed herein do not necessarily state or reflect those of the United States Government or any agency thereof.

By acceptance of this article the publisher acknowledges that the U.S. Government retains a nonexclusive, irrevocable, and exclusive right in and to the copyright in the published form of this contribution or its translation in all forms and media for U.S. Government purposes.

The Los Alamos National Laboratory requests that the publisher identify this article as work performed under the auspices of the U.S. Department of Energy.

DISTRIBUTION OF THIS DOCUMENT IS UNLIMITED

**MASTER**  
**Los Alamos** Los Alamos National Laboratory  
Los Alamos, New Mexico 87545



## FIRST OPERATION OF THE LOS ALAMOS FREE-ELECTRON LASER OSCILLATOR\*

R. W. Warren, B. E. Newnam, W. E. Stein, J. G. Winston, R. L. Sheffield,  
M. T. Lynch, J. C. Goldstein, M. C. Whitehead, O. R. Norris,  
G. Luedemann, T. O. Gibson, and C. M. Humphry

Los Alamos National Laboratory  
Los Alamos, New Mexico 87545

### Abstract

An FEL oscillator has been operated at wavelengths between 9 and 11  $\mu\text{m}$  with a peak intracavity power of about 20 MW and an average output power of 1 kW in 70-ns pulses. We present the design parameters and operating characteristics. We report measurements of spontaneous emission, start-up of oscillations, and signal growth through  $\sim 9$  orders of magnitude to saturation. The dependence of gain and saturation on cavity length, alignment, beam parameters, and other critical variables are discussed and compared with theory.

### Introduction

The Los Alamos Free-Electron laser (FEL) recently has achieved oscillation in the spectral range from 9 to 11  $\mu\text{m}$ . The maximum in-cavity power was about 30 MW, while the peak and average extracted powers were 1 MW and 1 kW, respectively. These power levels and tuning range all exceed previously reported values. In contrast with the FEL oscillators operated at Stanford<sup>1,2</sup> and L.U.R.E. (Orsay),<sup>3</sup> the Los Alamos FEL has a short wiggler (1 m), operates at a high peak current (25 A), and employs a conventional rf linear accelerator rather than a superconducting structure or a storage ring. In the following sections, first we briefly review the operation of the accelerator and beamline. For a more complete discussion of the accelerator and its peripheral equipment we refer the reader to earlier publications.<sup>4,5</sup> The remainder of this paper is devoted to the optical results to which we compare our theoretical predictions.

### Accelerator

The major characteristics and parameters of the FEL oscillator system are listed in Table I; a plan view including the major components of the accelerator, the wiggler, and the optical cavity is shown in Fig. 1. The electron gun (Fig. 1, left side) produces a train of 2000 micropulses, spaced 46 ns apart, with a total duration of about 100 ns. This train of 2000 pulses, called the macropulse, passes through the wiggler generating spontaneous emission and, if conditions are right, stimulated emission, which grows exponentially to a saturated level of optical power. Each micropulse is emitted from the

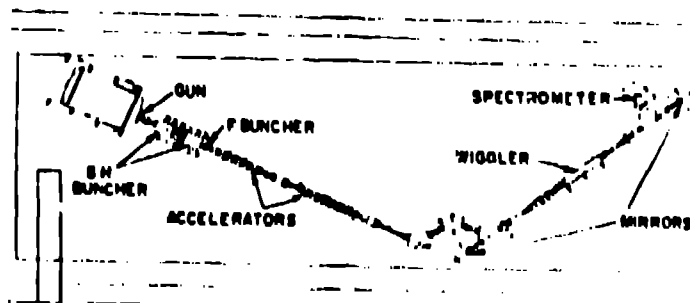


Fig. 1. Schematic of Los Alamos FEL oscillator system.

gun as a 2-A pulse about 3 ns long. Because the optical gain in the wiggler increases strongly with current, we have provided three bunchers<sup>6</sup> in the beamline to transform the micropulses into shorter pulses with higher currents. The first two subharmonic bunchers were not used for the initial experiments reported here because of technical problems. The combination of the final fundamental buncher and accelerator served to achieve a moderate ( $\times 10$ ) bunching so that the peak micropulse current reached  $\sim 25$  A. Without the subharmonic bunchers, however, each micropulse was complex, including a family

\*Work performed for Defense Advanced Research Projects Agency under the auspices of the US Department of Energy.

TABLE 1  
FEL OSCILLATOR PARAMETERS

<u>Wiggler</u>	
Length	100 cm
Period	2.73 cm
Gap between magnets	0.88 cm
Field strength	0.31 T
<u>Optical</u>	
Cavity length	6.92 m
Rayleigh range	63.2 cm
Diameter at waist	2.8 mm
Wavelength	9-11 $\mu\text{m}$
Round-trip losses	3.3%
Output coupler	3.0%
<u>Electron Beam</u>	
Electron energy	20-23 MeV
Accelerator Frequency	1.3 GHz
Micropulse width, estimated	30 ps
Peak current, estimated	25 A
Micropulse repetition time	46.15 ns
Macropulse length	100 $\mu\text{s}$
Energy spread	$\sim 2\%$ (FWHM)
Emittance	$\sim 2\text{ mm}^2\text{mrad}$
Diameter at waist	2.0 mm

of about five components (as shown in Fig. 2), each of which could oscillate independently of the others. These components are separated by 0.77 ns and appear to be about 0.5 ns wide. Their widths are actually much less, about 30 ps, but are broadened by the limited frequency response of the current monitor and oscilloscope. There are several disadvantages with this kind of micropulse, for example, lower peak currents and greater beam loading of the accelerator. However, some advantages resulted: in particular, the opportunity to examine the onset and saturation of oscillation for the different members of the family under identical conditions except for the difference in current.

As shown in Fig. 1, the accelerator is divided into two sections, each with separate control of amplitude and phase. The accelerator is required to capture the charge provided the buncher, to accelerate the charge to about 20 MeV without significant loss, to provide a small energy-spread and emittance, and to accomplish all this without significant deviation during the 2000 micropulses in a macropulse. Our measurements showed that that these goals were accomplished. About one-third of the charge leaving the gun reached the wiggler, a part being rejected at the accelerator's entrance and another part being purposely rejected at the scraper of Fig. 1 because of its low energy. Electron beam measurements also indicated that the energy spread was about 2% FWHM, with a transverse emittance of  $2\text{ mm}^2\text{mrad}$ . Figure 3 shows a measurement of beam energy

versus time during the macropulse. This display was produced by the slow deflector and energy spectrometer combination<sup>7</sup> of Fig. 1. Figure 3 shows that the peak energy and energy spread remained relatively constant during the 100- $\mu\text{s}$  macropulse, except for a short-lived transient at its beginning.



Fig. 2. Electron-current micropulse oscillogram revealing its multicomponent structure. Horizontal scale: 1 ns/cm; vertical scale: 0.5 A/cm.

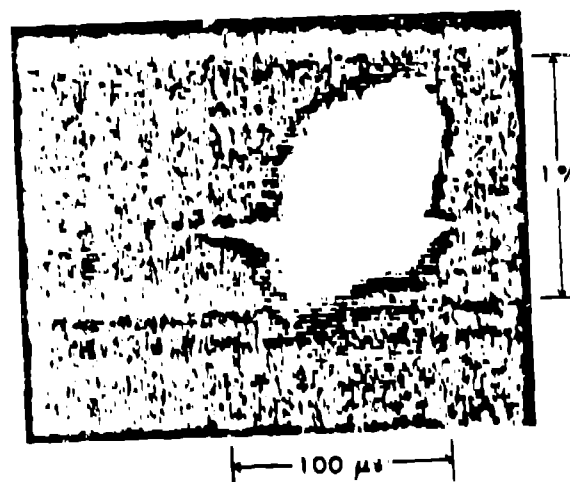


Fig. 3. Electron spectrometer measure of temporal dependence of energy spread during a macropulse. The bright horizontal line is an artifact caused by the fluorescent screen design. Some distortion of the energy distribution was produced by the TV screening system.

Of even more concern than energy spread and emittance is the regularity of the arrival time of the micropulses at the wiggler. There were effectively two clocks in the experiment: (1) the oscillator that drove the accelerator and determined the electron bunch arrival time, and (2) the light pulse reflecting back and forth between the mirrors. For optimum performance, these two clocks must beat with the same frequency and with a fixed phase difference throughout each macropulse. We attempted to provide this constancy by employing a stable crystal-controlled oscillator and by mounting the mirrors of the optical cavity on sturdy supports. Difficulties were encountered, that is, phase noise, which will be discussed below.

### Wiggler

A 1-m-long, permanent-magnet, plane-polarized wiggler was used in these experiments (Table 1). Except for its uniform 2.73-cm period, that is, no taper, it was identical to that used in previous studies.<sup>4,5</sup>

### Optical System

The optical cavity was about 6.9 m long with a round-trip time for optical pulses matching the electron micropulse separation of 46.15 ns. Its two mirrors are curved to form a stable resonator, with a fundamental mode of the right size to maximize the gain of the wiggler. This mode can be described by its Rayleigh range of 0.6 m. The mirrors were composed of multiple dielectric layers deposited on ZnSe substrates transparent to visible light. This combination allowed use of a HeNe laser beam for mirror alignment. The respective reflectances of the end mirror and output coupler were 99.7 and 97.0%.

The mirrors were remotely tilted for optimum alignment, and one mirror was translated longitudinally to achieve the correct spacing. The correct alignment was determined with an interferometer technique using a HeNe laser. This laser also was used to align the electron beam on the axes of the wiggler and optical cavity as previously described.<sup>4,5</sup> A separate HeNe interferometer monitored the mirror spacing continuously. The correct spacing was determined by a series of successive approximations. First, we measured the separation with a steel tape measure, achieving a precision of  $\pm 2$  mm. Next, we injected a 1-ns CO<sub>2</sub>-laser pulse through the end mirror and monitored the output through the output mirror as the pulse reflected back and forth between the mirrors. Figure 4 shows an example of the measured output. Two interesting features are evident: first, the pulse decayed exponentially, indicating the expected round-trip cavity loss of 3%. Second, the pulse decay was strongly amplitude modulated with a period about eight times the pulse spacing. This modulation was caused by a slight off-axis injection of the CO<sub>2</sub> pulse. An off-axis pulse of this kind will "walk" transversely across the faces of the mirrors, oscillating around their common axis with a period that we calculate to be eight round trips--in agreement with the observations. Our optical detector obviously was sensitive to the position of the walking pulse.

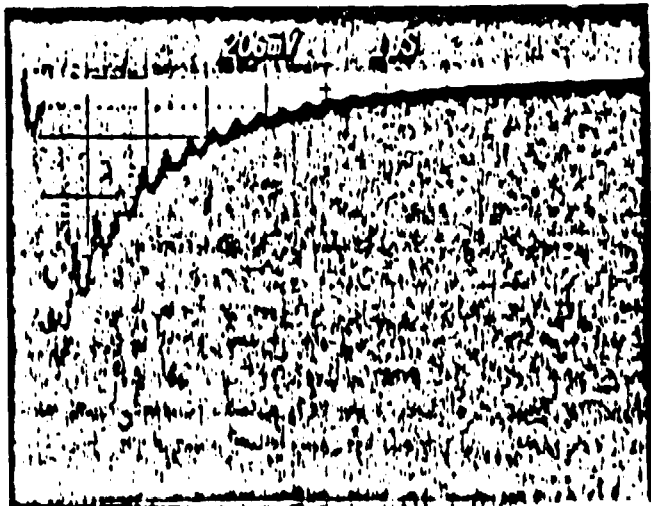


Fig. 4. Temporal decay of 10.6- $\mu$ m energy at the output of the oscillator cavity. The periodic structure resulted from slight off-axis injection of a single 1-ns CO<sub>2</sub>-laser pulse.

The injected CO<sub>2</sub> pulse also was used to measure the cavity length by adding the signal shown in Fig. 4 to a 108-MHz sine wave, a submultiple of the 1.3-GHz frequency used to drive the accelerator. If the optical cavity has the correct length, an oscillogram will show every echo of the injected CO<sub>2</sub> pulse superposed on the 108-MHz sine wave with exactly the same phase relationship. Figure 5 shows an example of this composite signal. By examining several hundred echoes in this way, the cavity length was adjusted with a precision of  $\pm 0.5$  mm. The final length adjustment was made by searching for evidence of stimulated emission.

### Optical Results

Our most sensitive optical detector was a mercury-doped, liquid helium-cooled germanium detector connected through two 5-GHz amplifiers in series to a 1-GHz oscilloscope display (Tektronix 7104). This detector was used directly to view the spontaneous emission from the electron beam and, with attenuators and filters of various kinds, to monitor the growing and

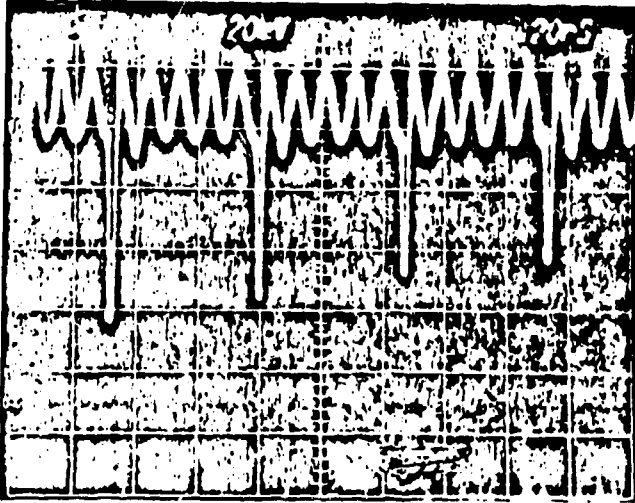


Fig. 5. Superposition of the decaying CO<sub>2</sub>-laser pulse exiting the oscillator cavity and the 108-MHz accelerator master oscillator.

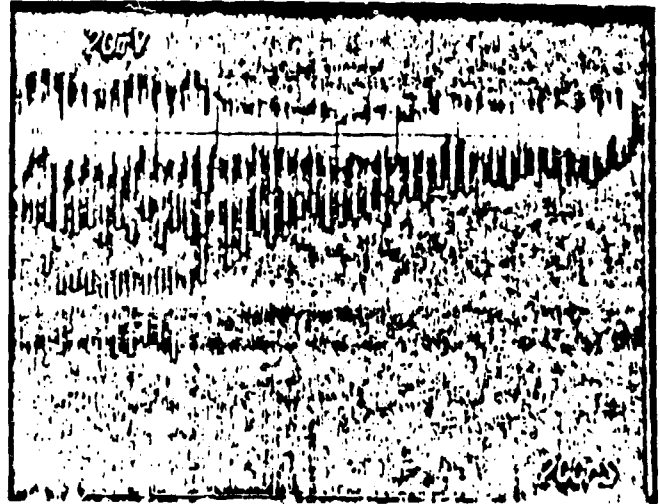


Fig. 6. Temporal decay of 10- $\mu$ m spontaneous emission from the oscillator cavity after the end of the macropulse of current.

saturated stimulated emission at 10  $\mu$ m, as well as various harmonics of 10  $\mu$ m. Figure 6 shows the spontaneous emission measured near the end of the 100- $\mu$ s macropulse. It shows a short train of pulses produced by the beam and afterwards, an exponentially decaying train of echoes. Although the noise level of these measurements is high, a crude measurement of the cavity loss could be obtained from the decay region. Normally, we verified low cavity losses in this way before attempting to find the correct cavity length.

As the correct length was approached, sporadic bursts of oscillation were observed. Figure 7 shows spontaneous emission on a compressed time scale where the whole macropulse is displayed. Clearly shown within the macropulse is an interval of temporary oscillation. When the cavity length was finally optimized, oscillation occurred during the whole macropulse, and saturation was established within 10-0  $\mu$ s at power levels  $10^9$  times above spontaneous emission. Figure 8 shows an example of the measurements we obtained. Superimposed on Fig. 8 is shown the optical power that theoretically would develop if the optical gain were 4, 8, and 16%. Clearly, the observed behavior agrees qualitatively with these curves in time to saturation and saturated power, but disagrees markedly in uniformity of the saturated power. This discrepancy will be discussed further below.

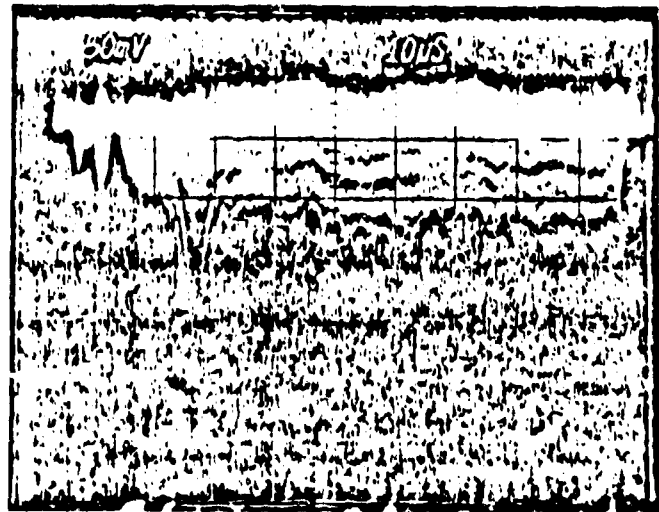


Fig. 7. Spontaneous 10- $\mu$ m emission during the macropulse of current revealing the threshold for stimulated emission.

During the early-growth stage of the emission, the optical gain fluctuates widely in the manner noted above for the saturated power. Figure 9 shows the maximum growth we have observed during this stage. This growth corresponds to a net growth of 17% per pass and a gross value (including the cavity loss of 3%) of 20%. Figure 9 also shows the growth, at a lower rate, of some members of the micropulse family that had lower current. The trailing end of a saturated macropulse of optical pulses is shown in Fig. 10. The exponential decay of pulse amplitude clearly reveals the 3% cavity loss, caused almost entirely by transmission through the output mirror.

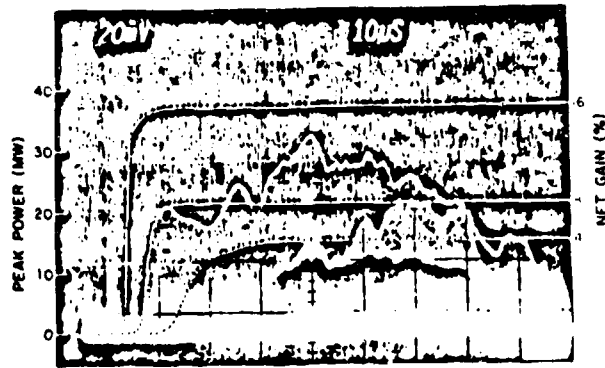


Fig. 8. Temporal variation of stimulated emission output power near saturation for the several micropulse-current components. Theoretical curves are plotted for comparison. Accuracy of the vertical power scale is within  $\pm 25\%$ .

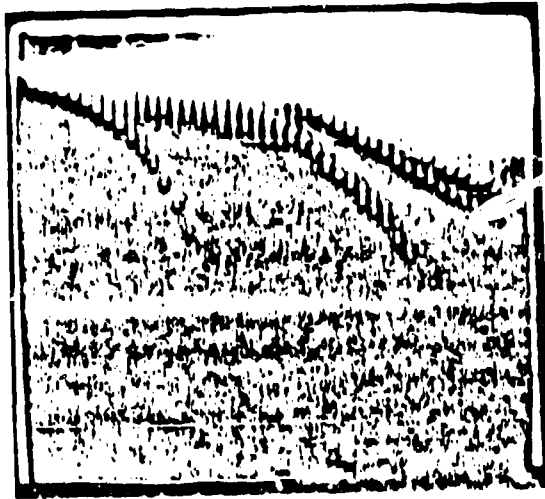


Fig. 9. Temporal build-up of laser oscillation for the several micropulse-current components.

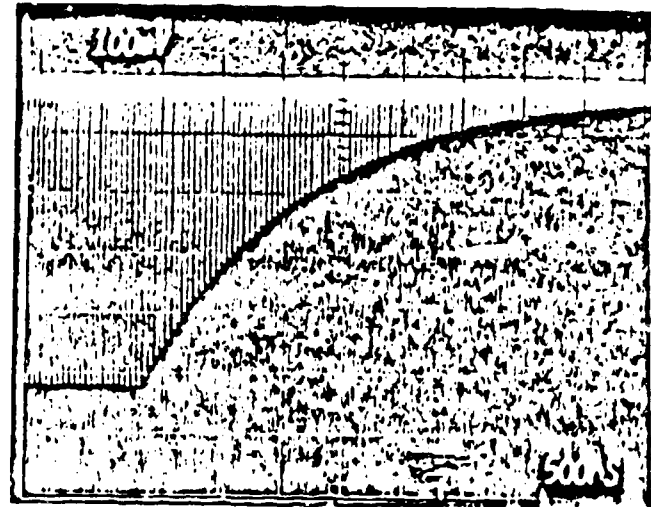


Fig. 10. Temporal decay of 10- $\mu\text{m}$  energy at the oscillator exit after the end of the macropulse of current.

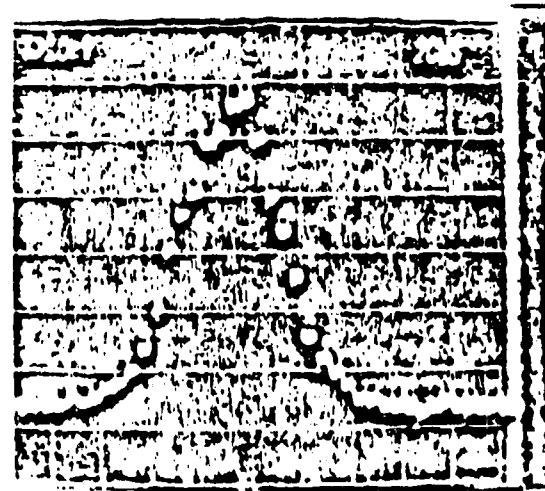


Fig. 11. Spatial profile (1-D) of the temporally integrated laser output. Beam diameter at  $1/e^2$  level is 15.5 mm.

Two important properties of a laser beam are its mode quality and its spectral harmonic content. Measurements were made of the spatial profile of our extracted laser beam, Fig. 11, using a multielement pyroelectric array, from which we determined that the beam was composed mainly of the fundamental Gaussian mode. When we purposely tipped the cavity mirrors, however, we stimulated the walking motion of the optical beam discussed above. This behavior can be described as the generation of a mixture of the two lowest order cavity modes. Figure 12 is an oscillogram, like Fig. 10, of the trailing end of a macropulse showing an amplitude modulation that results from this walking motion.

The second and third harmonics of 10  $\mu\text{m}$  were observed as well during oscillations. Besides their different wavelengths, they were characterized by different decay behavior in the cavity. Multilayer mirrors composed of quarter-wave-thick films like ours reflect strongly only at odd harmonics of their design wavelength. Thus, the third harmonic generated during oscillation is trapped within the cavity and leaks out slowly, like the fundamental, but at a different rate. In contrast, the second harmonic is not trapped

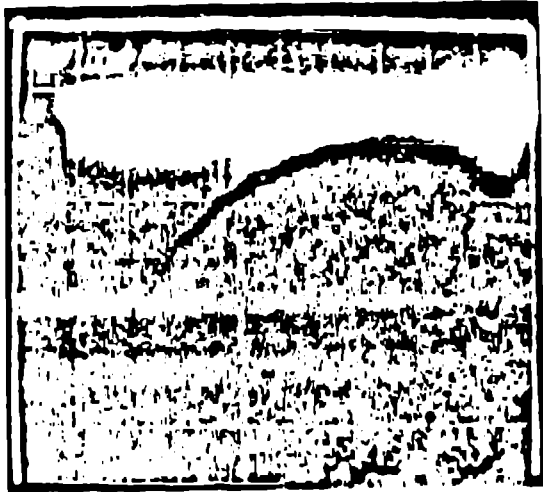


Fig. 12. Postlasing temporal decay of 10- $\mu$ m energy at the oscillator exit when cavity mirrors were intentionally misaligned.

maximum, measured small-signal gain (see Fig. 9) was 20%, in good agreement with this theory. The approximate magnitude, as well as the fluctuations in the saturation characteristics shown in Fig. 8, is in qualitative agreement with this as well as a second calculation in which we assumed that the phase of the accelerator was modulated sinusoidally around the correct phase with a period of 10  $\mu$ s and an amplitude of 5°. This modulation simulates a real, more random, modulation that we believe is caused by phase noise in our master oscillator.

Another important feature of our experimental results, which has been compared with theory, is the spatial profile of the light pulse. The measured widths at the  $1/e$  and  $1/e^2$  points were 11.5 and 15.5 mm in both the x- and y-directions. The ratio of these widths, 1.35, is in good agreement with 1.414, the theoretical value for a Gaussian shape. The absolute values agree with the theoretical widths within better than 10%, but at the present time this comparison cannot be made more precise without a better knowledge of the wavelength generated in this first series.

#### Summary

This paper is a report of our initial experimental results that must yet be augmented by some crucial information, that is, spectral data. These data are also plagued with gain fluctuations that we believe to be associated with phase errors in our master oscillator. The FEL oscillators operated at Stanford and L.U.R.E. escaped this noise problem because of the special features of superconducting accelerators and storage rings, respectively. We are now attempting to identify and correct our problem. Within these limitations, our results are in good agreement with theoretical predictions and no anomalous behavior has been observed.

#### Acknowledgments

We wish to thank those who have helped design and construct the apparatus, in particular, J. S. Fraser, T. A. Swann, J. E. Sollid, A. C. Saxman, A. H. Lumpkin, C. Friedrichs, P. J. Tallerico, and P. M. Giles. We also wish to acknowledge the inspirational leadership of C. A. Brau and the continued support and encouragement of J. M. Watson.

#### References

1. D. A. G. Deacon, L. R. Elias, J. M. J. Madey, G. J. Ramian, H. A. Schwettman, and T. J. Smith, "First Operation of a Free-Electron Laser," *Phys. Rev. Lett.* **38**, 892 (1977).
2. C. E. Hess, J. E. Edighoffer, G. R. Neil, T. I. Smith, and H. A. Schwettmann, "Tapered Wiggler Oscillator Results," to be published in *Proc. of Int. Conf. on Lasers '83* (San Francisco), 1984.

within the cavity but dies immediately when the electron beam is turned off. We have observed both behaviors: a 15%/pass loss for the third harmonic and instantaneous extinction for the second harmonic.

The high reflectivity region of our mirrors extends from 9 to 11  $\mu$ m. Oscillation within this range was accomplished easily by varying the electron beam energy by  $\pm 5\%$ .

#### Theoretical Comparison

A comparison of theory with experiment is complicated by the irregularity of the gain with time and by our lack of knowledge concerning the shape and peak current of the electron beam in the wiggler. We assume that the current pulse is Gaussian in shape and 30 ps wide. With these assumptions, our peak current was about 25 A. We will test this shape-assumption later with the help of the fast deflector.<sup>7</sup> However, preliminary calculations show that for this peak current, for an energy spread of 2%, and for an emittance of  $2\pi$  mm $\cdot$ rad, the small signal gain should be 16% and should have saturation characteristics as shown in the curve labeled "16%" of Fig. 8. The

3. M. Dillardon, P. Elleaume, J. M. Ortega, C. Bazin, M. Berger, M. Velghe, Y. Petroff, D. A. G. Deacon, K. E. Robinson, and J. M. J. Madey, "First Operation of a Storage-Ring Free-Electron Laser," *Phys. Rev. Lett.* 51, 1652 (1983).
4. R. W. Warren, B. E. Newnam, J. G. Winston, W. E. Stein, L. M. Young, and C. A. Brau, "Results of the Los Alamos Free-Electron Laser Experiment," *IEEE J. Quantum Electron.* QE-19, 391 (1983).
5. R. W. Warren, J. S. Fraser, W. E. Stein, J. G. Winston, T. A. Swann, A. H. Lumpkin, R. L. Sheffield, J. E. Sollid, B. E. Newnam, C. A. Brau, and J. M. Watson, "The Los Alamos Free-Electron Laser Oscillator Experiment: Plans and Present Status," in *Free-Electron Generators of Coherent Radiation*, C. A. Brau and M. O. Scully, Eds., SPIE Vol. 453, to be published, Feb. 1984.
6. J. S. Fraser, "Subharmonic Buncher for the Los Alamos Free-Electron Laser Oscillator Experiment," *ibid.*
7. R. L. Sheffield, W. E. Stein, A. H. Lumpkin, R. W. Warren, and J. S. Fraser, "Electron Beam Diagnostics for the Los Alamos Free-Electron Laser Oscillator Experiment," *ibid.*